










Global patterns of nitrate isotope composition in rivers and adjacent aquifers reveal reactive nitrogen cascading

Ioannis Matiatos ^{1✉}, Leonard I. Wassenaar¹, Lucilena R. Monteiro ¹, Jason J. Venkiteswaran ², Daren C. Gooddy ³, Pascal Boeckx ⁴, Elisa Sacchi ⁵, Fu-Jun Yue⁶, Greg Michalski⁷, Carlos Alonso-Hernández⁸, Christina Biasi ⁹, Lhoussaine Bouchaou^{10,11}, Nandana V. Edirisinghe¹², Widad Fadhullah¹³, Joseph R. Fianko¹⁴, Alejandro García-Moya⁸, Nerantzis Kazakis¹⁵, Si-Liang Li⁶, Minh T. N. Luu¹⁶, Sakhila Priyadarshane¹², Viviana Re ^{5,24}, Diego S. Rivera ¹⁷, Asunción Romanelli¹⁸, Prasanta Sanyal¹⁹, Fredrick Tamoo²⁰, Duc A. Trinh²¹, Wendell Walters²² & Nina Welti²³

Remediation of nitrate pollution of Earth's rivers and aquifers is hampered by cumulative biogeochemical processes and nitrogen sources. Isotopes ($\delta^{15}\text{N}$, $\delta^{18}\text{O}$) help unravel spatio-temporal nitrogen(N)-cycling of aquatic nitrate (NO_3^-). We synthesized nitrate isotope data ($n = 5200$) for global rivers and shallow aquifers for common patterns and processes. Rivers had lower median NO_3^- ($0.3 \pm 0.2 \text{ mg L}^{-1}$, $n = 2902$) compared to aquifers ($5.5 \pm 5.1 \text{ mg L}^{-1}$, $n = 2291$) and slightly lower $\delta^{15}\text{N}$ values ($+7.1 \pm 3.8\text{‰}$, $n = 2902$ vs $+7.7 \pm 4.5\text{‰}$, $n = 2291$), but were indistinguishable in $\delta^{18}\text{O}$ ($+2.3 \pm 6.2\text{‰}$, $n = 2790$ vs $+2.3 \pm 5.4\text{‰}$, $n = 2235$). The isotope composition of NO_3^- was correlated with water temperature revealing enhanced N-cascading in warmer climates. Seasonal analyses revealed higher $\delta^{15}\text{N}$ and $\delta^{18}\text{O}$ values in wintertime, suggesting waste-related N-source signals are better preserved in the cold seasons. Isotopic assays of nitrate biogeochemical transformations are key to understanding nitrate pollution and to inform beneficial agricultural and land management strategies.

¹ Isotope Hydrology Section, International Atomic Energy Agency, Vienna, Austria. ² Department of Geography and Environmental Studies, Wilfrid Laurier University, Waterloo, ON, Canada. ³ British Geological Survey, Wallingford, Oxfordshire, UK. ⁴ Isotope Bioscience Laboratory, Ghent University, Ghent, Belgium. ⁵ Department of Earth and Environmental Sciences, University of Pavia, Pavia, PV, Italy. ⁶ School of Earth System Science, Tianjin University, Tianjin, China. ⁷ Department of Earth, Atmospheric and Planetary Sciences, Department of Chemistry, Purdue University, West Lafayette, IN, USA. ⁸ Departamento de Estudio de la Contaminación Ambiental, Centro de Estudios Ambientales de Cienfuegos, Cienfuegos, Cuba. ⁹ University of Eastern Finland, Kuopio, Finland. ¹⁰ Laboratory of Applied Geology and Geo-Environment, Faculty of Sciences, Ibn Zohr University, Agadir, Morocco. ¹¹ International Water Research Institute, Mohammed VI Polytechnic University, Benguérir, Morocco. ¹² Isotope Hydrology Section, Sri Lanka Atomic Energy Board, Orugodawatta, Wellampitiya, Sri Lanka. ¹³ School of Industrial Technology, Universiti Sains Malaysia, George Town, Penang, Malaysia. ¹⁴ Department of Nuclear Sciences and Applications, School of Nuclear and Allied Sciences University of Ghana/Ghana Atomic Energy Commission, Accra, Ghana. ¹⁵ Aristotle University of Thessaloniki, School of Geology, Thessaloniki, Greece. ¹⁶ Analytical Chemistry Department, Institute of Chemistry Vietnam Academy of Science and Technology A18, Hanoi, Vietnam. ¹⁷ CisGER, Universidad del Desarrollo, Las Condes, Chile. ¹⁸ National Scientific and Technical Research Council (CONICET) - National University of Mar del Plata (UNMdP), Mar del Plata, Argentina. ¹⁹ Indian Institute of Science Education and Research, Kolkata, Mohanpur, India. ²⁰ Department of Zoological Sciences, Kenyatta University, Nairobi, Kenya. ²¹ Nuclear Training Center, Vietnam Atomic Energy Institute, Hanoi, Vietnam. ²² Brown University, Providence, RI, USA. ²³ CSIRO Agriculture and Food, Urrbrae, SA, Australia. ²⁴ Present address: Earth Sciences Department, University of Pisa, Pisa, Italy. ✉email: i.matiatos@iaea.org

The exponential growth of the human population concomitant with intensive development of fertilized agricultural and industrial activity since the 1950s caused sharp increases in nitrogen loadings to rivers and surficial aquifers worldwide^{1,2}. Dissolved reactive nitrogenous species (e.g., NO_3^- , NH_4^+) are prevailing pollutants in many rivers and aquifers, stemming primarily from agricultural activities, municipal waste sources, and combustion derived nitrogen (N) deposition³. The impact of reactive nitrogenous species on water and ecosystems (e.g., eutrophication, hypertrophication) and human health (e.g., methemoglobinemia, cancer, thyroid disease)^{4–6} occurs in series, known as N-cascading¹, and is of existential concern.

The global nitrogen cycle is a subject of considerable debate and concern that anthropogenic loadings are driving it beyond Earth's natural resilience boundaries⁷. Reactive nitrogen cascades through aquatic ecosystems differentially¹, since some systems accumulate N, whereas others transform it through diverse biogeochemical N-cycling processes like nitrification, denitrification, N_2 -fixation, dissimilatory nitrate reduction (DNRA), ammonification, and biological assimilation at rates dependent on the environmental conditions. These complexities make it difficult to unravel what point-based NO_3^- concentrations in rivers or their connected aquifers embody at any point in time, apart from regulatory pollutant exceedances, and quantitative knowledge of the roles of N-cycling processes in the terrestrial aquatic environments remains deficient.

Stable isotopes of NO_3^- ($\delta^{15}\text{N}$, $\delta^{18}\text{O}$) are used, particularly in the last decades, to help identify the sources of high N-pollution in aquatic systems^{8–12}. Contemporary preparative and isotope techniques enable fast low-cost isotopic analysis of $^{15}\text{N}/^{14}\text{N}$ and $^{18}\text{O}/^{16}\text{O}$ ratios to ppb concentrations to incorporate comparative isotopic information from pristine aquatic environments¹³, and references therein]. Distinctive $\delta^{15}\text{N}$ and $\delta^{18}\text{O}$ biplot clusters were initially proposed to “assign” organic and inorganic NO_3^- origins^{3,14,15}, however, NO_3^- sources rarely exhibit unique combinations of nitrogen (N) and oxygen (O) isotopic values as shown by ambiguous or widely overlapping clusters (e.g., soil, manure/sewage, NH_4^+ fertilizer), which make straightforward assignments problematic. Accordingly, others^{16–18} recommend including additional isotopes (e.g., $\delta^{11}\text{B}$), other chemicals (e.g., pharmaceuticals, food additives), and/or biological markers (e.g., chlorophyll-*a*, fecal coliforms) to better differentiate sources of nitrogen pollution in freshwaters, particularly as related to municipal sewage, animal waste, industrial and atmospheric sources.

One common misperception in the interpretation of NO_3^- isotopes in aquatic systems is that its isotopic composition is a conservative tracer of N source(s), despite isotope fractionations during numerous biogeochemical transformations that significantly alter the $\delta^{15}\text{N}$ and $\delta^{18}\text{O}$ values of nitrate¹⁹. Instead, the $\delta^{15}\text{N}$ and $\delta^{18}\text{O}$ of NO_3^- in aquatic systems are more frequently a mixture of time and seasonally dependent N-source (s) and cumulative isotopic fractionations that occur during transport and biogeochemical transformation of dissolved N-species^{20–22}. It is well-known that biological nitrate uptake (assimilation) and denitrification processes preferentially process the light isotopes, resulting in heavy isotope enrichment of residual nitrate¹⁴. Despite uncertainties in the assessment of sources of nitrate pollution using $\delta^{15}\text{N}$ and $\delta^{18}\text{O}$, these stable isotopes retain fundamental source and process information to help decipher the complexity of N-biogeochemistry in aquatic environments^{21,23,24}.

Common patterns of N-cycling processes using global spatial data sets of NO_3^- and its stable isotopes are established for soils and plant matter^{25–28}, but larger-scale spatiotemporal studies of nitrate in rivers and adjacent aquifers are lacking^{20,29–31}. Here we

synthesized global river and adjacent shallow aquifer nitrate isotope (^{15}N and ^{18}O of NO_3^-) data sets from the scientific literature as well as new data ($n = \sim 5200$) to (a) provide a first-order global assessment of spatiotemporal patterns of NO_3^- and its isotopes in rivers and aquifers and (b) evaluate whether NO_3^- transformations are impacted by key environmental factors, such as temperature, climate, and seasonality. The investigation of the origin of nitrate pollution in rivers and groundwater at the local scale usually requires a deeper consideration of additional information such as N flux information from homogenized land-use types³²; however, the detailed local evaluation was beyond the scope of this work. This synthesis provides a global foundational perspective to evaluate the potential and limitations of nitrate stable isotopes to track nitrogen pollution sources in aquatic systems, especially rivers, and to promote a data-based framework for further improving our understanding of the transformation mechanisms of nitrogen for sustainable management and remediation of N-contaminated waters.

Results

Overall assessment of global river and groundwater nitrate data sets. Concentrations of nitrate in rivers and adjacent aquifers deviated from normal distributions and were highly skewed (skewness index > 2), hence median values were retained³³. Of all samples, rivers had substantively lower median NO_3^- concentrations ($0.3 \pm 0.2 \text{ mg L}^{-1}$, $n = 2902$) compared to groundwater ($5.5 \pm 5.1 \text{ mg L}^{-1}$, $n = 2291$) (Supplementary Table 1). Around 2% of river water samples exceeded the WHO (World Health Organization) threshold of 50 mg L^{-1} (as NO_3^-), whereas in groundwater the exceedance was far higher ($\sim 34\%$). The Kruskal–Wallis test indicated that nitrate concentration differences between rivers and groundwater subsets were significant (p -value < 0.05) (Supplementary Table 2).

The distribution patterns for $\delta^{15}\text{N}$ and $\delta^{18}\text{O}$ of NO_3^- in rivers and groundwater deviated from normal distributions (Supplementary Fig. 1). The isotope data were not as skewed as NO_3^- concentrations (skewness index < 2 for the number of records > 300 ³³), hence average values were retained to compare these isotope variables among them. Outliers were mostly extreme values falling within the upper and lower tails of the distributions of the Quantile–Quantile (Q–Q) plots (Supplementary Fig. 1). The $\delta^{15}\text{N}$ values of nitrate in rivers were slightly lower ($+7.1 \pm 3.8\%$, $n = 2902$) than aquifers ($+7.7 \pm 4.5\%$, $n = 2291$, p -value < 0.05). Kendall¹⁴ presented an early compilation of nitrate isotope data in aquatic systems and reported groundwater nitrate has considerably higher $\delta^{15}\text{N}$ values than rivers, however, others found more positive $\delta^{15}\text{N}$ nitrate values in surface waters than nearby groundwater¹⁵. Other case studies affirmed higher mean $\delta^{15}\text{N}$ values for NO_3^- in shallow groundwater compared to local rivers in urban waters (Manila, Bangkok, and Jakarta)³⁴ or under different land-use-based catchments¹². Overall, the $\delta^{18}\text{O}$ values of nitrate in rivers and groundwaters worldwide were indistinguishable from each other ($+2.3 \pm 6.2\%$, $n = 2790$, vs $+2.3 \pm 5.4\%$, $n = 2235$, p -value > 0.05 , respectively) (Supplementary Tables 1 and 2).

Isotope variation with latitude. The global data set included river and groundwater samples spanning from 67° N to 38° S LAT and from 145° E to 123° W LON (Fig. 1). There were more samples between 30° N to 60° N than other latitudinal ranges, reflecting the preponderance of data from North America, Europe, and East Asia. However, Central Asia, Central, and South America, Oceania, and Africa are poorly represented for nitrate isotope data sets due to a lack of water N pollution studies in those areas. The $\delta^{15}\text{N}$ and $\delta^{18}\text{O}$ of nitrate were negatively correlated with latitude for rivers ($\delta^{15}\text{N}\text{-NO}_3^- = -0.07 \pm 0.01 \times \text{Latitude} + 10.14 \pm 0.46$,

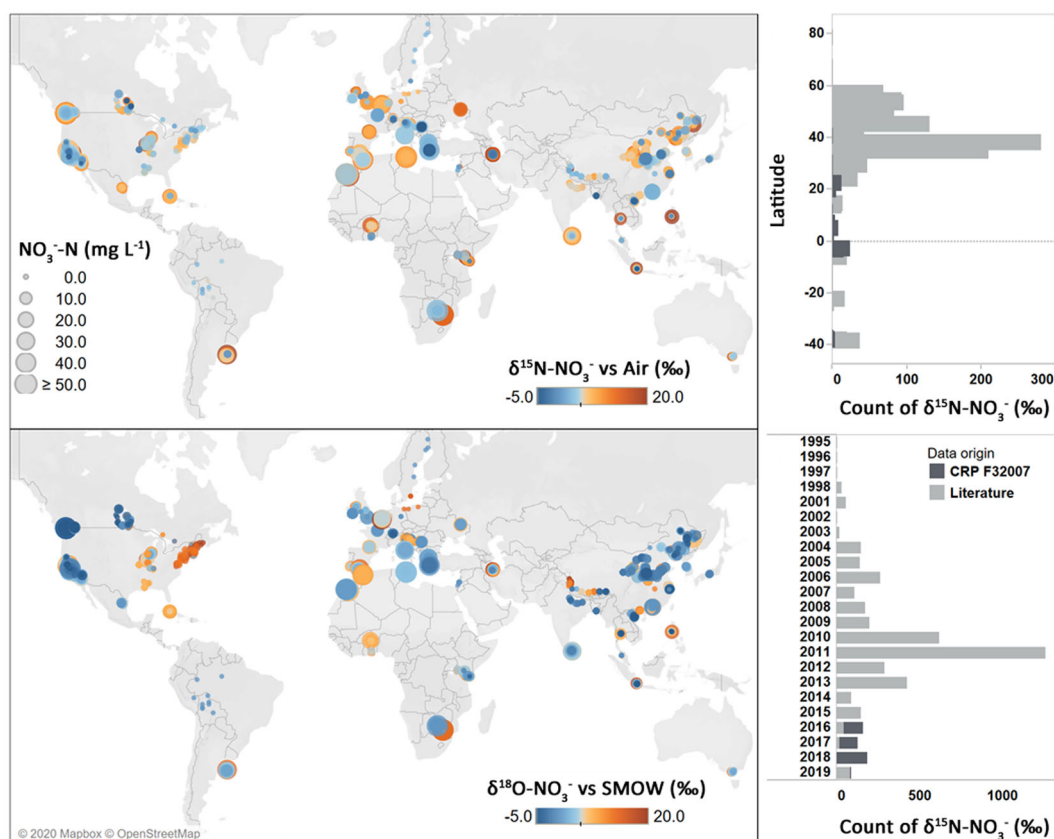


Fig. 1 Geographical distribution of $\delta^{15}\text{N}$ and $\delta^{18}\text{O}$ data for nitrate in river water and groundwater by number (#) of measurements by 0.1° latitude and year of sample collection. The size of each circle corresponds to the concentration of NO_3^- -N in mg L^{-1} . The light and dark gray bars indicate the data were retrieved from literature or the IAEA Coordinated Research Project (CRP), respectively. Most data were from 30° N and 60° N LAT and between 2010 and 2013.

p -value < 0.05 , $n = 521$, $R^2 = 0.07$; $\delta^{18}\text{O}-\text{NO}_3^- = -0.12 \pm 0.02 \times \text{Latitude} + 9.47 \pm 0.79$, p -value < 0.05 , $n = 506$, $R^2 = 0.06$) and groundwater ($\delta^{15}\text{N}-\text{NO}_3^- = -0.15 \pm 0.03 \times \text{Latitude} + 14.59 \pm 1.16$, p -value < 0.05 , $n = 301$, $R^2 = 0.08$; $\delta^{18}\text{O}-\text{NO}_3^- = -0.30 \pm 0.03 \times \text{Latitude} + 16.05 \pm 1.43$, p -value < 0.05 , $n = 299$, $R^2 = 0.18$) (Supplementary Fig. 2 and Supplementary Table 3). When data from the Northern Hemisphere were considered separately, the correlation between $\delta^{15}\text{N}$ and $\delta^{18}\text{O}$ of NO_3^- and latitude yielded a similar regression slope and intercept.

Relationship between ^{15}N and ^{18}O of NO_3^- . Both river and groundwater nitrate revealed positive correlations between the $\delta^{18}\text{O}$ and $\delta^{15}\text{N}$ values (Fig. 2). The $\delta^{18}\text{O}$ of NO_3^- was weakly but significantly correlated with $\delta^{15}\text{N}$ for rivers ($\delta^{18}\text{O}-\text{NO}_3^- = 0.64 \pm 0.03 \times \delta^{15}\text{N}-\text{NO}_3^- - 2.51 \pm 0.26$, p -value < 0.05 , $n = 2445$, $R^2 = 0.13$) and groundwater ($\delta^{18}\text{O}-\text{NO}_3^- = 0.43 \pm 0.02 \times \delta^{15}\text{N}-\text{NO}_3^- - 0.99 \pm 0.21$, p -value < 0.05 , $n = 2172$, $R^2 = 0.13$). However, river waters had a significantly (p -value < 0.05) higher regression slope (0.64 ± 0.03) compared to groundwater (0.43 ± 0.02) (Fig. 2).

The influence of ^{18}O in water and molecular O_2 on the ^{18}O of NO_3^- produced during nitrification is typically described using a simple isotope mass balance¹⁴:

$$\delta^{18}\text{O}-\text{NO}_3^- = 2/3 \times \delta^{18}\text{O}-\text{H}_2\text{O} + 1/3 \times \delta^{18}\text{O}-\text{O}_2 \quad (1)$$

Eq. (1). Studies investigating nitrification in aquatic systems found the $\delta^{18}\text{O}$ of NO_3^- does not necessarily conform to this model, even when the $\delta^{18}\text{O}$ of O_2 is assumed constant or in equilibrium with air³⁵ ($+23.5$ – $+24.2\%$). To reduce the

influence of $\delta^{18}\text{O}$ from local water contributing to nitrate during its transformations, we normalized the $\delta^{18}\text{O}-\text{NO}_3^-$ to the $\delta^{18}\text{O}-\text{H}_2\text{O}$ values from the same water sample wherever possible (i.e., “relative to in situ H_2O ” instead of “relative to SMOW”)³¹. The normalization to in situ water ^{18}O resulted in an improved but weak correlation between $\delta^{18}\text{O}-\text{NO}_3^-$ vs H_2O and $\delta^{15}\text{N}-\text{NO}_3^-$ for river waters ($\delta^{18}\text{O}-\text{NO}_3^-$ vs $\text{H}_2\text{O} = -0.21 \pm 0.02 \times \delta^{15}\text{N}-\text{NO}_3^- - 0.33 \pm 0.19$, $R^2 = 0.09$, p -value < 0.05 , $n = 946$) and groundwater ($\delta^{18}\text{O}-\text{NO}_3^-$ vs $\text{H}_2\text{O} = -0.10 \pm 0.02 \times \delta^{15}\text{N}-\text{NO}_3^- - 1.17 \pm 0.06$, $R^2 = 0.15$, p -value < 0.05 , $n = 1138$). The slopes of the “normalized” regression became negative and decreased from ~ 0.6 to ~ 0.2 for rivers and from ~ 0.4 to ~ 0.1 for aquifers. The river water samples from warmer tropical areas (e.g., Kenya, Ghana, Thailand) drove slopes to more negative $\delta^{18}\text{O}$ and higher $\delta^{15}\text{N}$ values. Results of the least-square linear regression analyses of the isotopic variables for river water and groundwater subsets are summarized in Supplementary Table 4.

Variation of nitrate isotopic composition with water temperature. Water temperature (T_w) is often used as a proxy for potential rates of the microbial activity or primary productivity and was used to consider its relationship to the isotopic composition of NO_3^- in rivers and aquifers^{36,37}. In this assessment, the temperature was the river or groundwater temperature at the time of sampling without further considering overall climatic or seasonal aspects. Detailed results of least-square linear regression analyses of the nitrate isotopic variables for river water and groundwater are depicted in Supplementary Table 5. The $\delta^{15}\text{N}$ of NO_3^- in rivers showed a weak but significant positive correlation

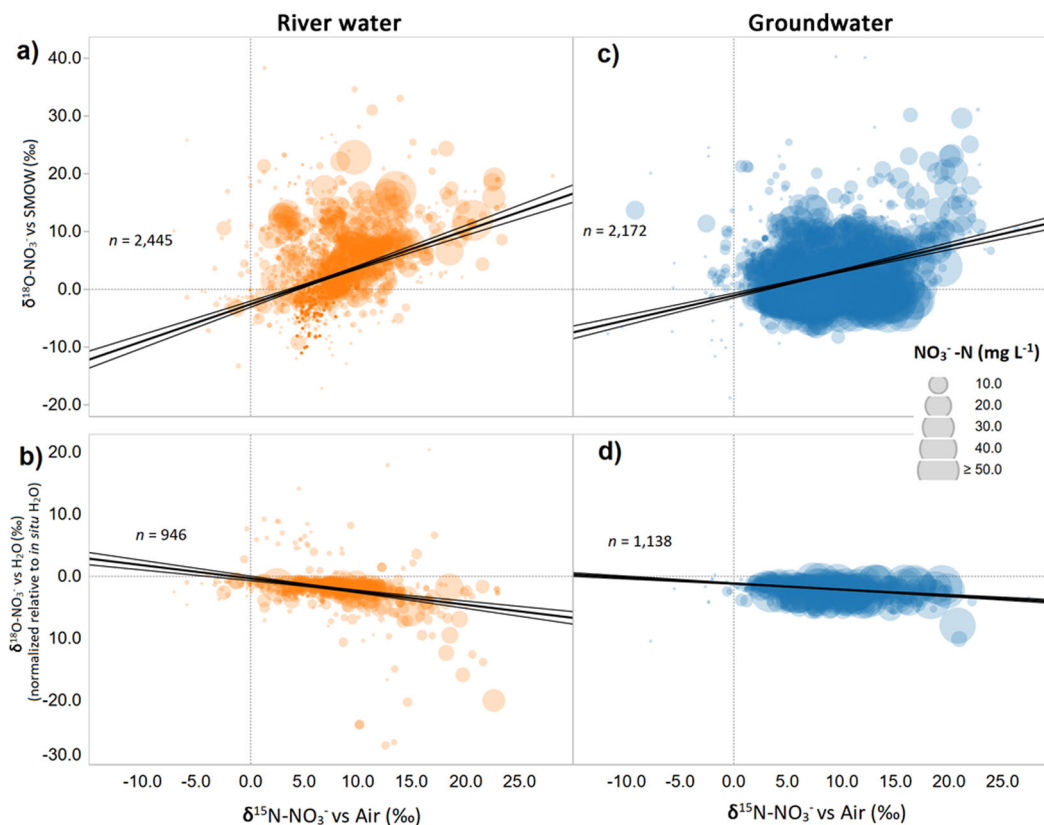


Fig. 2 $\delta^{18}\text{O}$ vs $\delta^{15}\text{N}$ of NO_3^- in rivers and groundwater. Symbol size denotes NO_3^- concentration in mg L^{-1} . The $\delta^{18}\text{O}$ values are relative to SMOW and normalized to in situ H_2O , as described in Venkiteswaran et al.³¹. The results of the linear regression models of panels a–d are in Supplementary Table 4.

with T_w ($\delta^{15}\text{N}-\text{NO}_3^- = 0.12 \pm 0.04 \times T_w + 6.55 \pm 0.82$, $R^2 = 0.03$, p -value < 0.05 , $n = 253$), but for groundwater, there was no correlation ($\delta^{15}\text{N}-\text{NO}_3^- = 0.05 \pm 0.05 \times T_w + 8.45 \pm 1.03$, $R^2 = 0.01$, p -value > 0.05 , $n = 189$) (Fig. 3). The $\delta^{18}\text{O}$ of NO_3^- in rivers had a weak but significant positive correlation with T_w ($\delta^{18}\text{O}-\text{NO}_3^- = 0.10 \pm 0.04 \times T_w + 5.19 \pm 0.90$, $R^2 = 0.02$, p -value < 0.05 , $n = 275$), whereas in groundwater the correlation was very strong ($\delta^{18}\text{O}-\text{NO}_3^- = 0.48 \pm 0.04 \times T_w - 3.79 \pm 0.95$, $R^2 = 0.41$, p -value < 0.05 , $n = 170$). Regressions against T_w using in situ normalized ^{18}O nitrate values were conducted and resulted in less variable and slightly negative non-zero slopes like Fig. 2.

Seasonal variation of stable isotopes of NO_3^- . To investigate the effect of seasonality on the isotopic composition of nitrate in rivers and groundwater, we used data from temperate climates (C), given that seasonality is strong in this climatic zone compared to the others (see “Methods” section, Fig. 4). The mean $\delta^{15}\text{N}$ values of nitrate in rivers showed no difference between spring and fall ($+6.9 \pm 3.6\text{‰}$, $n = 583$ to $+6.7 \pm 2.6\text{‰}$, $n = 606$, p -value > 0.05), but a $\sim 1\text{‰}$ increase in $\delta^{15}\text{N}$ in winter compared to all other seasons ($+7.7 \pm 3.8\text{‰}$, $n = 200$, p -value < 0.05). The average $\delta^{18}\text{O}$ values of nitrate in rivers revealed a $\sim 2\text{‰}$ decrease from spring to autumn (from $+2.2 \pm 5.9\text{‰}$, $n = 530$ to $-0.1 \pm 4.5\text{‰}$, $n = 562$, p -value < 0.05), and a $\sim 4.5\text{‰}$ increase from autumn to winter (from $-0.1 \pm 4.5\text{‰}$, $n = 562$ to $+4.4 \pm 4.5\text{‰}$, $n = 149$, p -value < 0.05).

Shallow aquifers showed no $\delta^{15}\text{N}$ seasonality (p -value > 0.05) in mean NO_3^- between spring, summer, autumn, and winter ($+7.8 \pm 4.4\text{‰}$, $+7.7 \pm 3.9\text{‰}$, $+8.1 \pm 3.8\text{‰}$, and $+8.1 \pm 3.5\text{‰}$, respectively). The average $\delta^{18}\text{O}$ of NO_3^- in groundwater was similar in summer, autumn, and winter ($+0.6 \pm 4.8\text{‰}$, $+0.6 \pm 4.6\text{‰}$, and $+0.1 \pm 3.3\text{‰}$, respectively) but was $\sim 2\text{‰}$ higher in spring ($+2.1$

$\pm 6.0\text{‰}$, $n = 268$, p -value < 0.05) compared to all other seasons. However, considering that groundwater replenishment usually takes place in the wet period (October–April) in the northern hemisphere, we examined the difference in the isotopic values between the high recharge period and the low recharge period (May–September). There was no significant difference in $\delta^{15}\text{N}$ and $\delta^{18}\text{O}$ of NO_3^- between the two periods, although the $\delta^{18}\text{O}$ of NO_3^- was slightly lower in the high recharge period (Supplementary Fig. 3). No clear-cut pattern was observed for the relationship between $\delta^{15}\text{N}$ and NO_3^- in rivers or groundwater by season to confirm single predominant biogeochemical processes, including denitrification¹⁴ (Supplementary Fig. 4).

Variation of stable isotopes of NO_3^- with climate. The average $\delta^{15}\text{N}$ of nitrate in rivers was significantly higher ($\sim 3.0\text{‰}$) in tropical (A) ($+10.2 \pm 5.1\text{‰}$, $n = 137$) vs temperate (C) ($+7.5 \pm 3.7\text{‰}$, $n = 834$) or cold (D) ($+7.4 \pm 4.0\text{‰}$, $n = 252$) climates (Fig. 5). The same pattern was observed for $\delta^{18}\text{O}$ of NO_3^- for rivers, having ~ 2 – 3‰ higher values in tropical (A) ($+6.6 \pm 5.9\text{‰}$, $n = 137$) vs temperate (C) ($+4.4 \pm 5.4\text{‰}$, $n = 722$) and cold (D) ($+3.8 \pm 5.6\text{‰}$, $n = 275$) climates. Arid climates (B) showed significantly higher $\delta^{15}\text{N}$ values for nitrate ($+8.9 \pm 6.0\text{‰}$, $n = 74$) compared to temperate (C) or cold climate (D), but similar $\delta^{18}\text{O}$ values for nitrate ($+5.5 \pm 8.1\text{‰}$, $n = 74$) compared to other climate types. However, the arid climate zone had fewer data compared to the other climate types due to a limited number of river water nitrate studies in those climates.

The shallow aquifers had the lowest $\delta^{15}\text{N}$ values in temperate (C) ($+7.8 \pm 4.1\text{‰}$, $n = 986$) and arid (B) climates ($+7.3 \pm 4.1\text{‰}$, $n = 522$) and the highest in tropical/equatorial (A) ($+8.9 \pm 5.5\text{‰}$, $n = 44$) and cold (D) climates ($+9.0 \pm 5.2\text{‰}$, $n = 24$). However, these differences were indistinguishable (p -value > 0.05), hence no

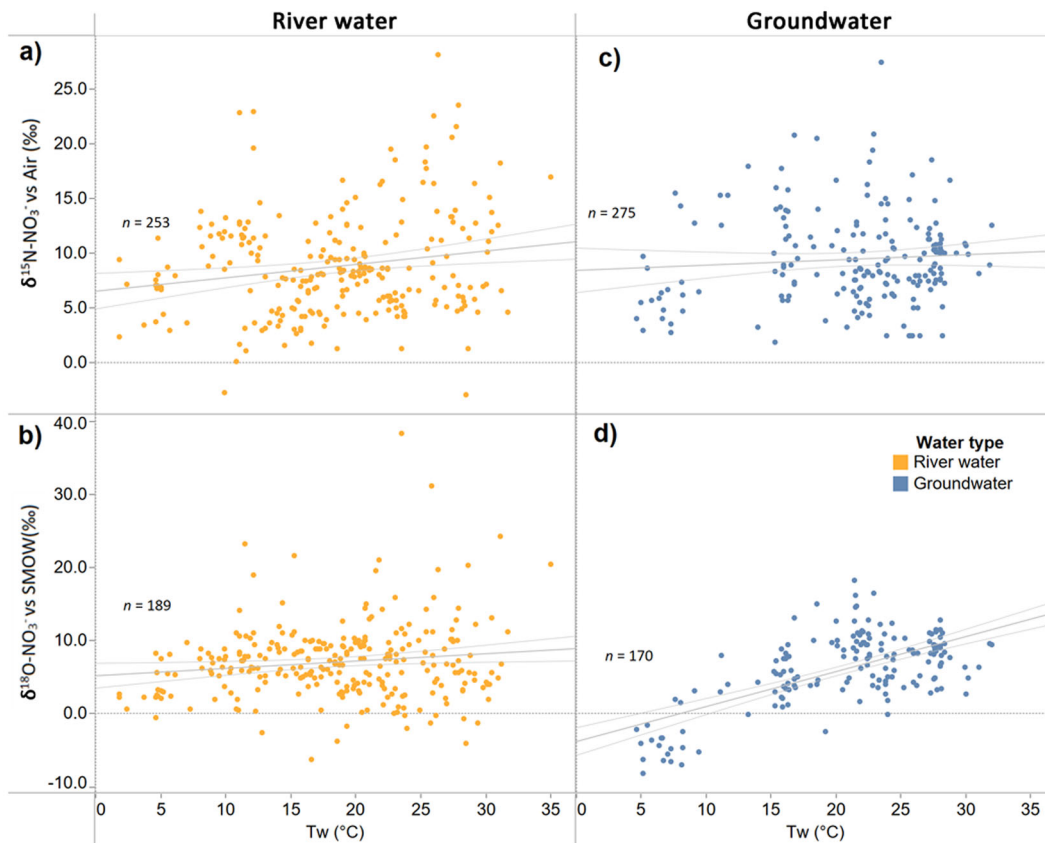


Fig. 3 Variation of $\delta^{18}\text{O}$ and $\delta^{15}\text{N}$ of NO_3^- in river waters and groundwater with water temperature (T_w) in $^\circ\text{C}$. The linear regression of $\delta^{18}\text{O}-\text{NO}_3^-$ (‰) vs T_w ($^\circ\text{C}$) was more significant for groundwater ($R^2 = 0.41$) than river waters ($R^2 < 0.02$). The results of the linear regression models for panels **a-d** are in Supplementary Table 5.

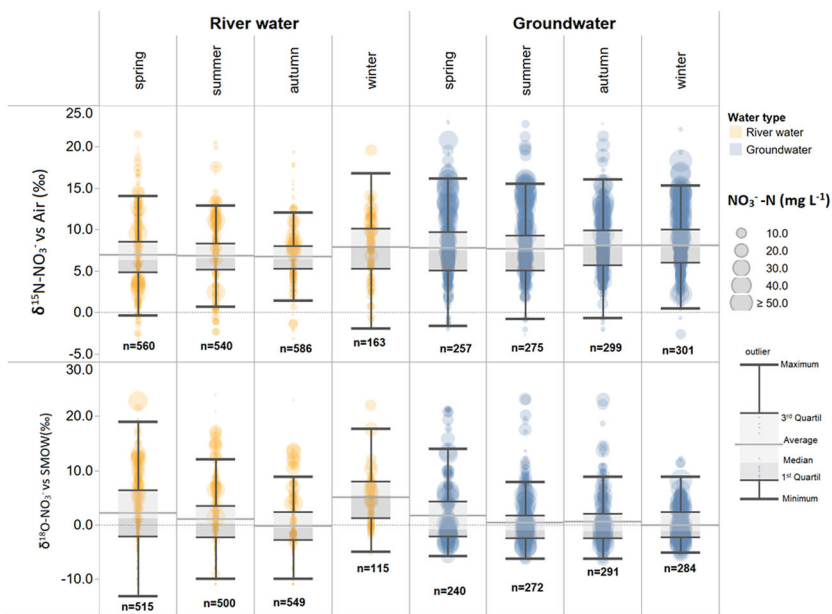


Fig. 4 Variation of $\delta^{15}\text{N}$ and $\delta^{18}\text{O}$ of nitrate in rivers and groundwater classified by season. The symbol size expresses the $\text{NO}_3^- \text{-N}$ in mg L^{-1} . Higher average $\delta^{15}\text{N}$ and $\delta^{18}\text{O}$ values in river water nitrate are found in winter. Error bars show average (gray line), median (light to dark gray division), 1st and 3rd quartile, and whiskers extend to 1.5 interquartile range.

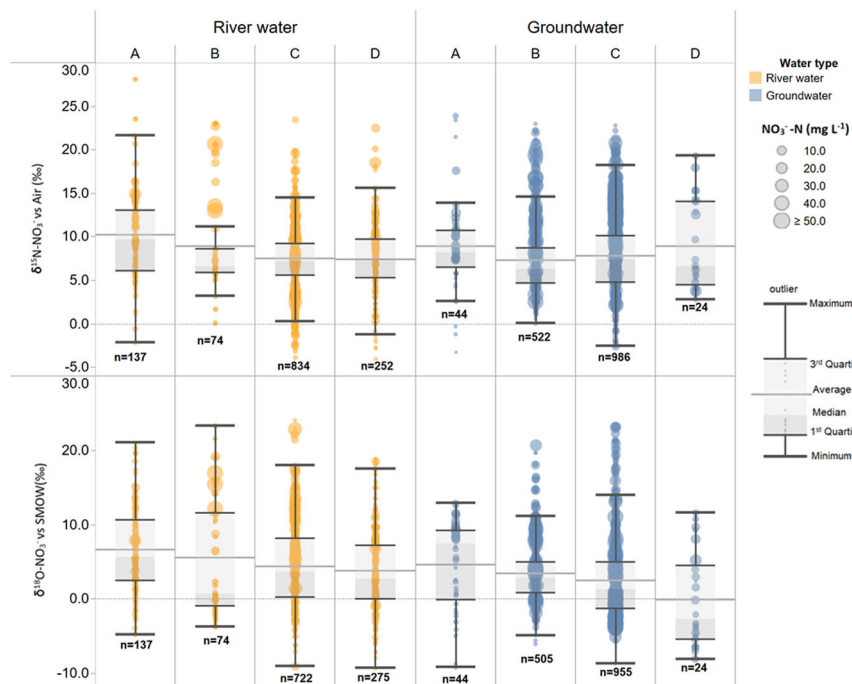


Fig. 5 Variation of $\delta^{15}\text{N}$ and $\delta^{18}\text{O}$ of NO_3^- in rivers and groundwater by climate. A: Tropical/Equatorial, B: Arid, C: Temperate, D: Cold. Symbol size expresses the NO_3^- -N concentration (mg L^{-1}). Tropical climates had the highest $\delta^{15}\text{N}$ and $\delta^{18}\text{O}$ values for nitrate in rivers. Error bars show average (gray line), median (light to dark gray division), 1st and 3rd quartile, and whiskers extend to 1.5 interquartile range.

N-isotopic impact solely from climate could be found. Groundwater nitrate $\delta^{18}\text{O}$ values exhibited the same pattern as rivers, with lower $\delta^{18}\text{O}$ values in cold (D) climates ($-0.1 \pm 6.4\text{‰}$, $n = 24$), that differed significantly from those in tropical (A) ($+4.6 \pm 6.0\text{‰}$, $n = 44$) climates. The average $\delta^{18}\text{O}$ of NO_3^- values in arid (B) ($+3.4 \pm 4.0\text{‰}$, $n = 505$) and temperate (C) ($+2.5 \pm 4.9\text{‰}$, $n = 505$) climates were significantly different from the other two climate types. Cold climates had fewer $\delta^{15}\text{N}$ and $\delta^{18}\text{O}$ records for groundwater compared to the other three climate types, which could bias this result. Rivers and groundwater showed no clear-cut relationship between $\delta^{15}\text{N}$ and NO_3^- by climate type (Supplementary Fig. 5).

Discussion

The lower median NO_3^- concentrations in rivers compared to adjacent shallow aquifers can be explained by the decrease of agricultural N inputs at the industrialized countries of the Northern hemisphere due to more severe fertilization regulations, whereas many aquifers do not yet exhibit decreasing nitrate contents. This is due to much longer mean residence times for N in the unsaturated zone and the aquifer³⁸, which is controlled by several factors such as the thickness and hydro-lithological characteristics of the unsaturated zone, the spatiotemporal variations in recharge rate, and the diffusive and dispersion processes through the nitrogen stock in the soil and the unsaturated zones. The lower median NO_3^- concentrations in rivers can also be explained by a complex combination of riparian and in situ attenuation and uptake by biological productivity, seasonal dilution (e.g., runoff, snowmelt), differential baseflow connectivity, and long-term dispersion processes, which lowers the ambient NO_3^- concentration in rivers. Given that NO_3^- sources are difficult to “fingerprint” using only stable isotopes, we suggest that the notable differences in NO_3^- concentrations between river waters and adjacent aquifers are attributable to unique locational differences in in situ N-cycling processes. As microbes have low biomass in most groundwater systems, NO_3^-

attenuation, and cycling is achieved by closed-system nitrification and denitrification and uncommonly by DNRA or anammox^{29,39}. Shallow aquifers are the recipients of NO_3^- transport from residual leaching from soils and the unsaturated zone, where NH_4^+ and other nitrogenous compounds are favorably oxidized but can also be adsorbed or reduced depending on soil retention capacity^{40–43}. Pronounced denitrification effects have been reported for some unconfined aquifers^{30,44,45}.

Regression analysis of $\delta^{18}\text{O}$ vs $\delta^{15}\text{N}$ for river waters and groundwater generated slopes suggesting an “apparent” denitrification trend (~ 0.5)^{3,31}. However, denitrification is unlikely to be the only process for the observed $\delta^{18}\text{O}:\delta^{15}\text{N}$ slope, which is expected to be canonical under closed-system conditions⁴⁶. The lack of a clear pattern between the isotopes and NO_3^- concentration indicates that multiple processes that recycle nitrogen occur in river water systems. Granger and Wankel¹⁹ proposed that the deviations from the canonical slope of 1 for denitrification can be due to concurrent NO_3^- production catalyzed by nitrification and/or anammox.

A non-zero normalized slope suggests that H_2O was not the only factor controlling the oxygen isotopic composition of nitrate (Eq.1). The large decrease in the slopes of the regression after normalization for in situ water confirmed a strong dependence of $\delta^{18}\text{O}$ of NO_3^- on the $\delta^{18}\text{O}$ of water when the NO_3^- is formed by oxidation of nitrite or ammonium⁴². However, in situ water normalizations do not consider potential large daily or seasonal variations in the $\delta^{18}\text{O}$ of in situ gaseous or dissolved O_2 ³⁵ involved in the N-cycling processes. Thus, the observed negative deviations of the slopes from “zero” suggest an influence of $\delta^{18}\text{O}-\text{O}_2$ on the isotopic composition of nitrate. The latter may be more profound for rivers than aquifers. Investigations of $\delta^{18}\text{O}-\text{O}_2$ in productive rivers show a preponderance of lower $\delta^{18}\text{O}$ values (as low as $+3.4\text{‰}$), particularly during the growing season due to photosynthetic processes^{35,47,48}. Tropical rivers typically show high rates of primary production, all-year-round growth, and less seasonal variation in solar irradiance than temperate latitudes⁴⁹.

On a diel basis, $\delta^{18}\text{O}\text{-O}_2$ is lowest during the day due to the production of DO by photosynthesis from substrate water, whereas during the night $\delta^{18}\text{O}\text{-O}_2$ can be higher than the atmospheric equilibrium value due to preferential consumption of light O_2 by respiring organisms with inward diffusion of isotopically heavy O_2 from the atmosphere⁵⁰. Thus, the negative in situ normalized slopes of the $\delta^{18}\text{O}$ regression line for rivers suggest some influence of ^{18}O depleted O_2 , especially for highly productive rivers where oxygen supersaturation and $^{18}\text{O}_2$ depletion and nitrification coexist. But even if the $\delta^{18}\text{O}\text{-O}_2$ contribution was considered as a fixed atmospheric constant, any kinetic and equilibrium isotope fractionation during oxygen exchange between H_2O and NO_2^- before final oxidation to NO_3^- may also result in deviations from a 2:1 mixing ratio line ($\delta^{18}\text{O}\text{-H}_2\text{O}:\delta^{18}\text{O}\text{-O}_2$)⁴². Therefore, the relationship between $\delta^{18}\text{O}\text{-NO}_3^-$ and $\delta^{18}\text{O}\text{-H}_2\text{O}$ can be used to detect isotope fractionation effects related to the incorporation of oxygen atoms during ammonia oxidation to nitrite (NO_2^-), which readily exchanges oxygen atoms with in situ water during the oxidation of the latter to nitrate⁵¹. Conversely, for aquifers the $\delta^{18}\text{O}\text{-O}_2$ values in recharge zone gas often deviate from the air (+23.5‰), but mostly in a positive direction up to >+39‰ as soil O_2 is consumed by microbial respiration^{52,53}. The substantial variability in the $\delta^{18}\text{O}$ of NO_3^- associated with nitrification is also dependent on soil and water properties and is also a function of residence time⁵⁴.

The difficulty to elaborate clear relationships between ^{18}O of H_2O , O_2 , and NO_3^- is also due to the temporal variability of the oxygen variables and underscores the need for further investigations to better understand N-dynamics related to cycling. Unfortunately, oxygen isotope normalization processes that consider all potential reactive oxygen pools (e.g., in situ H_2^{18}O and $^{18}\text{O}_2$) involved in N-cycling processes have not been fully investigated to our knowledge⁵⁵. New studies measuring $\delta^{18}\text{O}\text{-NO}_3^-$ and $\delta^{18}\text{O}\text{-H}_2\text{O}$ and $\delta^{18}\text{O}\text{-O}_2$ in the same water are therefore required to better explain the patterns and variations of the oxygen isotope composition of nitrate in rivers and groundwater.

The $\delta^{15}\text{N}$ and $\delta^{18}\text{O}$ of NO_3^- in rivers showed a positive correlation with T_w likely reflecting the influence of higher microbial activity and productivity with temperature and thus the biogeochemical N processing rates. Higher $\delta^{15}\text{N}$ values in rivers are likely driven by enhanced N-cascading. This means that due to increased temperature, metabolic rates accelerate, which progressively enriches ^{15}N in NO_3^- compared to its source signature¹⁴. Average $\delta^{15}\text{N}$ values of nitrate >7‰ typically suggest that nitrogen has undergone multiple recycling after its initial fixation from N_2 (either biological or Haber-Bosch), as these processes bring reactive N in the plant-soil-water continuum with a ^{15}N value of ~0‰⁵⁶. An observed weak positive correlation of $\delta^{18}\text{O}\text{-NO}_3^-$ with T_w and a negative correlation with latitude suggests that ambient $\delta^{18}\text{O}\text{-H}_2\text{O}$ has some impact on nitrate isotope values.

The pattern of decreasing $\delta^{15}\text{N}\text{-NO}_3^-$ in rivers with latitude agrees with the N isotopic climatic patterns observed for soil organic matter (SOM)²⁵. The pattern of higher $\delta^{15}\text{N}\text{-NO}_3^-$ values with the water temperature in rivers is observed from cold (D) to tropical (A) climates. Amundson et al.²⁵ observed a weakly positive correlation between soil organic matter (SOM) $\delta^{15}\text{N}$ and Mean Annual Temperature (MAT) (slope = 0.13, $R^2 = 0.11$, p -value < 0.1, $n = 85$) for arid and tropical zones. A decrease in SOM $\delta^{15}\text{N}$ with lower MAT was seen at sites between about 10–40 degrees North or South albeit with a smaller data set (slope = -0.08, $R^2 = 0.09$, p -value < 0.04, $n = 49$)²⁷. Craine et al.²⁶ observed a positive trend of SOM $\delta^{15}\text{N}$ with MAT (slope = 0.18, p -value < 0.001, MAT > 9.8 °C) and a negative correlation

with Mean Annual Precipitation (MAP) at a global scale that was attributed to soil and organic matter properties²⁶. Martinelli et al.²⁸ reported higher values for $\delta^{15}\text{N}$ in N-rich soils and foliage from tropical forests compared to temperate forests. Brookshire et al.⁵⁷ suggests that higher MAT enhances soil N-cycling as seen by ^{15}N enrichment in soil organic matter and the NO_3^- concentration of tropical rivers.

The seasonality of $\delta^{15}\text{N}$ and $\delta^{18}\text{O}$ of nitrate in temperate rivers showed a pattern of isotopic enrichment of nitrate in spring and summer compared to autumn, which could be attributed to higher biological assimilation in surface water systems in the warmer seasons⁵⁸. The $\delta^{15}\text{N}$ values during winter compared to other seasons appeared to more closely reflect mixing of multiple organic-pollutant N-sources (e.g., sewage wastes, urban, and livestock wastewaters)^{9,24} as a result of reduced application and leaching of fertilizers, and restricted microbial and primary productivity during the cold season⁵⁹. Additionally, in the cold season, the relative fraction of NO_3^- denitrified vs assimilated is higher, since increased N-loadings in winter or early spring runoff are often associated with high discharge events and snowmelt⁵⁷. Elevated $\delta^{18}\text{O}$ of NO_3^- during winter can also be attributed to $\delta^{18}\text{O}\text{-H}_2\text{O}$ and $\delta^{18}\text{O}\text{-O}_2$ variation combined with variable soil/water and land-use properties of the different catchments. For example, high $\delta^{18}\text{O}$ values in nitrate can be attributed to the influence of $\delta^{18}\text{O}\text{-O}_2$ (Eq.1), especially in respiration-influenced ecosystems⁴⁸, increased atmospheric NO_3^- deposition (>+30.0‰)¹⁴, especially during high discharge events, or artificial NO_3^- fertilizer (>20.0‰)¹⁴ mixed with nitrification-derived NO_3^- in soils and infiltrating pore waters, especially in agricultural areas⁵⁴. Full equilibration or O-isotope exchange of NO_2^- with H_2O before being oxidized to NO_3^- in soils, local respiration, and rapid redox cycling between NO_3^- and NO_2^- can also potentially increase $\delta^{18}\text{O}\text{-NO}_3^-$ values^{19,54,60}.

Shallow phreatic aquifers showed strongly dampened seasonal nitrate and isotopic variability compared to river waters. Given NO_3^- concentrations are generally buffered in aquifers over longer timeframes (e.g., years), the range of $\delta^{15}\text{N}$ values in groundwater reflect longer-term climatic and land-use changes or established processes taking place in the soil and the unsaturated zone before NO_3^- leaches into the groundwater system^{30,61}. The lack of a clear seasonal variation of $\delta^{15}\text{N}$ and $\delta^{18}\text{O}$ of NO_3^- in groundwater is attributed to nitrifying and mixing of nitrate sources introduced at different points or periods in time due to variable residence times (from months to years) in the unsaturated zone^{38,62}. There was no significant difference in $\delta^{15}\text{N}$ and $\delta^{18}\text{O}$ of NO_3^- between the high and low recharge periods, although the $\delta^{18}\text{O}$ of NO_3^- was slightly lower in the high recharge period. This could imply a change in recharge source water (e.g., snowmelt vs rains) or the ^{18}O of O_2 , which combined affect the ^{18}O values of microbially mediated nitrate. Because groundwater temperatures are usually stable and generally reflect MATs³⁷ (and in situ $\delta^{18}\text{O}_{\text{H}_2\text{O}}$ correlates with air temperature), it was unsurprising to see a correlation of $\delta^{18}\text{O}$ of NO_3^- with T_w . This suggests we cannot discount the possibility that ^{18}O variance of groundwater nitrate is controlled by additional processes or isotope fractionations affecting O_2 involved in soil and vadose zone nitrification⁵³. However, the relationship between $\delta^{18}\text{O}$ in nitrate with latitude showed the highest oxygen isotope values tended to be at the warmer tropical/equatorial climates and can be attributed to a systematic change in the $\delta^{18}\text{O}$ of associated H_2O (Eq.1) with decreasing latitude, continentality or altitude⁶³.

In summary, although rivers and shallow aquifers are primary and often well connected receiving environments for land-based anthropogenic N-pollution, shallow aquifers have five times higher median NO_3^- concentration than rivers, indicating that

NO_3^- is more persistent in aquifers and has long residence times, given lower microbial activity and a limited number of possible N-removal process mechanisms (e.g., denitrification). River waters and groundwater receive nitrate with $\delta^{15}\text{N}$ and $\delta^{18}\text{O}$ values spanning the expected natural and anthropogenic ranges (from -10‰ to $+26\text{‰}$ for $\delta^{15}\text{N}$ and -17‰ to $+25\text{‰}$ for $\delta^{18}\text{O}$)³, indicating a globally consistent suite of N-sources. We identified some global drivers of the isotopic variability of nitrate in rivers and groundwater, recognizing that this simplification required aggregating many possible diverse nitrate sources typically observed at the catchment or complicated by seasonal variability. A deeper analysis of latitude and climatic factors is recommended to better distinguish the role of soil properties, precipitation patterns, land-use, and agricultural practices. The $\delta^{18}\text{O}$ vs $\delta^{15}\text{N}$ relationships observed suggested combinations of multiple biogeochemical (e.g., nitrification, anammox) and mixing processes taking place in rivers and aquifers in different seasons, which are not easily distinguishable with infrequent or synoptic samplings. River water nitrate had higher $\delta^{15}\text{N}$ and $\delta^{18}\text{O}$ values in winter, suggesting a change in N-processing due to lowered temperatures and productivity and perhaps less alteration of the original isotopic composition of multiple organic-related N-sources. Across a wide range of global climate types, river waters and groundwater showed systematically higher $\delta^{15}\text{N}$ and $\delta^{18}\text{O}$ values in the arid and tropical/ equatorial climates, mirroring an increase in MAT. This relationship was also seen in the increase in $\delta^{15}\text{N}$ of nitrate in rivers and groundwater with decreasing latitude and the positive correlation between $\delta^{15}\text{N}$ and $\delta^{18}\text{O}$ with T_w .

We have provided a first-order attempt to identify global patterns in the isotopic composition of nitrate related to common environmental factors, such as climate and season impacting N-cascade-related processes in rivers and associated shallow groundwaters. Our findings highlight the importance of water temperature as a driving force of biogeochemical microbial activity and productivity in rivers, however, the impact on the $\delta^{15}\text{N}$ and $\delta^{18}\text{O}$ of nitrate differed when examined on a seasonal or on a climate basis. Our findings suggest that higher frequency or seasonal sampling of river water systems is of critical importance to better and more deeply understand annual N-pollution dynamics, and winter sampling appears to better reflect the N-isotopic signals of the anthropogenic sources of nitrate. Further investigations to study N-cycling in river waters at a higher frequency are urgently needed (e.g., seasonal, diel) and systematic data collections of nitrate, particularly from the southern hemisphere climate types, such as arid and polar, for which data are limited or absent, are strongly recommended. Recent technological advances in isotopic assays of nitrate have vastly reduced the analytical and cost barriers to conduct high-frequency $\delta^{15}\text{N}$ and $\delta^{18}\text{O}$ of nitrate. Other key parameters, such as DO, redox potential, labile organic material, and solar radiation should also be systematically measured or considered to help better understand the controlling factors of the N-transformations in river waters, especially on a seasonal basis. Measuring $\delta^{18}\text{O}$ of the water and dissolved oxygen from the same samples as $\delta^{18}\text{O}$ of NO_3^- will allow a better assessment of N-cycling processes in rivers and groundwater. Understanding the fate of nitrogen in aquifers and the connectivity to rivers requires a fuller local understanding of hydrogeological processes, such as water source, flow paths, and water residence times (e.g., ^3H tracers) that control nitrogen transit times and contribution to baseflow (e.g., retardation of N due to the recycling of N in organic matter and subsequent mineralization processes). Our synthesis affirms nitrate isotope techniques are useful to assess the origin of nitrogen pollution in rivers and groundwater. However, we caution that interpretations of nitrate isotopes may be complicated where nitrogen undergoes many biogeochemical transformations,

especially in productive systems, that can mask the original isotopic source signal. Examination of N-cascading aspects are critically important to inform the implementation of beneficial land and agricultural management strategies aiming at mitigating increasingly serious nitrogen pollution in Earth's rivers and aquifer systems. The clear isotopic linkage of the N-cascading in rivers to key climate parameters may have implications for future water quality management under changing climatic conditions.

Methods

Literature data collection. A literature search was conducted using online tools and bibliographic databases (e.g., Web of Science, Google Scholar, Scopus, etc.) for papers containing nitrate and isotope data from rivers and adjacent aquifers. We reported shallow aquifer data because many of the river studies contained data for adjacent aquifers owing to the possible connectivity of groundwater to riverine baseflow, although in most papers any connectivity of adjacent aquifers to the rivers was unconfirmed. Data compilations were restricted to journal articles where both $\delta^{15}\text{N}$ and $\delta^{18}\text{O}$ values of nitrate are available, and samples were then classified as River or Groundwater. Scientific papers focusing on precipitation, deep aquifers, soils, tap water, seawater, wastewater effluent, or artificial isotopic tracers were omitted. The list of cited data used is found in Supplementary References.

Data preparation. Established data preparation procedures resulted in a curated data set suitable for statistical analysis⁶⁴. Data were extracted from tables and supplementary materials, maps, and text (Supplementary Fig. 6). If the original work did not provide location coordinates, approximate latitude and longitude were obtained using Google Earth (<https://www.google.com/earth/>). The data assessment affirmed that NO_3^- was the species linked to the reported isotope ratios ($^{15}\text{N}/^{14}\text{N}$ and $^{18}\text{O}/^{16}\text{O}$) along with verification of units (as NO_3^- or -N) and concentration (e.g., mg L^{-1} , $\mu\text{mol L}^{-1}$, $\mu\text{g L}^{-1}$, etc.). Nitrate concentration data were converted to a common unit (mg L^{-1} -N) and sampling date format (e.g., 2016-03-01) (Supplementary Fig. 7). The $^{18}\text{O}/^{16}\text{O}$ of in situ H_2O associated with a nitrate sample, if available, was also included in the data set. The ratios of $^{15}\text{N}/^{14}\text{N}$ and $^{18}\text{O}/^{16}\text{O}$ of NO_3^- and $^{18}\text{O}/^{16}\text{O}$ of H_2O were reported in δ notation in units of per mille (‰), where $\delta = (R_{\text{sample}}/R_{\text{AIR}} \text{ or } \text{SMOW}} - 1)$ and R is the ratio of $^{15}\text{N}/^{14}\text{N}$ or $^{18}\text{O}/^{16}\text{O}$ in N_2 in atmospheric air (AIR) or Standard Mean Ocean Water (SMOW), respectively.

Seasons were identified separately for each Hemisphere (N vs S) using the reported sampling date (month) to ensure consistency. Each sample location was coded using the Köppen climatic classification⁶⁵. Due to limited data from high latitudes, river and groundwater data were classified into four climatic groups; A: Equatorial/Tropical climate, B: Arid climate, C: Temperate climate, D: Cold climate. Additional categorical and site information associated with the nitrate and isotopic data was obtained from the publications and is included in Supplementary Table 6. Important variables, such as Eh, dissolved O_2 (DO), dissolved organic nitrogen (DON), precipitation per catchment, Total Nitrogen (TN), that might contribute to a better understanding of the global N isotope variations of nitrate were either lacking or unavailable. For example, DO values were only available in 7.7% of the river waters data set and thus were excluded from further processing.

Data curation. Excessively high or suspicious values of NO_3^- and other N-species concentrations were verified by a careful review of the original paper. In some cases, authors were contacted to provide clarification. The $\delta^{15}\text{N}$ and $\delta^{18}\text{O}$ values of nitrate were sorted to avoid duplication from publications reusing the same data sets²⁶. Almost all groundwater data (~95%) was from adjacent shallow phreatic aquifers of <20 m depth below ground surface.

Final data set and analytical aspects. The data set comprised 5194 sample points from 70 papers (~86% of the whole data set, Supplementary References) plus new isotopic results. There were 2902 nitrate and associated isotope analyses from rivers and 2291 analyses from nearby shallow groundwater. Most samples were from between 2002 and 2016; fewer data exist from 1968 to 1990s due to analytical barriers particularly for $\delta^{18}\text{O}$ ⁶⁶.

A total of 374 new river water nitrate and isotope samples from 10 countries were analyzed in the IAEA Isotope Hydrology Laboratory using the Ti(III) reduction method¹³ to reduce nitrate to N_2O gas in septum vials. The N_2O in the headspace was measured for ^{15}N and ^{18}O using a CF-IRMS (Isoprime-100 Trace Gas Analyser). The analytical uncertainties were $\pm 0.2\text{‰}$ and $\pm 0.4\text{‰}$ for $\delta^{15}\text{N}/\delta^{18}\text{O}$, respectively. For Quality Control, the water samples, that do not give the expected N_2O yield on the IRMS based on the determined NO_3^- concentration, were repeated until they agree within 95% of the expected target before results are accepted. Oxygen isotopes ($\delta^{18}\text{O}_{\text{H}_2\text{O}}$) of the same water samples were analyzed by laser spectroscopy at the IAEA using a Los Gatos Research Liquid-Water Isotope Analyzer (TLWIA-912). The analytical uncertainty was ± 0.1 for $\delta^{18}\text{O}_{\text{H}_2\text{O}}$. Chemical analysis of new samples included nitrate following standard discrete analyser methods⁶⁷.

Statistical evaluation. To evaluate the data, graphical plots by sample type (river or groundwater) were employed along with frequency distribution diagrams (histogram, Q-Q plot, P-P plot, boxplot) and metrics such as Pearson skewness. To check for normality, Shapiro–Wilk, and Kolmogorov–Smirnov tests were applied. The mean and standard deviation (SD) were used to describe the variation of variables with a skewness index of <2, whereas median and the median absolute deviation (MAD) were used otherwise³³. A single-factor analysis of variance (ANOVA) and Kruskal–Wallis non-parametric analysis of variance were performed to determine if differences between the means or the medians of the groups were significant. A conventional probability value (*p*-value) of 0.05 was used to indicate significance for differences between river and groundwater and seasonal subsets⁶⁸.

A least-square linear regression model of type I was applied to investigate relationships between $\delta^{15}\text{N}$ and $\delta^{18}\text{O}$ of nitrate to other variables. The least-square linear regression type II was tested by assuming that the two isotopic variables ($\delta^{15}\text{N}$ and $\delta^{18}\text{O}$ in nitrate) were dependent⁶⁹. However, the difference in the slopes and intercepts were small in most cases (<10%), which allowed us to use model-I patterns for nitrate isotopes in both rivers and groundwaters. The results of regression models of type II are found in Supplementary Methods (Supplementary Tables 7–8 and Supplementary Figs. 8–15). All linear regression models were evaluated by examining the goodness of fit and significance of the slopes. All statistical tests were done using R v.3.3.2⁷⁰.

Data availability

The global data sets available from the publications or generated in this study are available from <https://nucleus.iaea.org/sites/ihn/Pages/GNIR.aspx>.

Received: 3 July 2020; Accepted: 11 January 2021;

Published online: 01 March 2021

References

- Galloway, J. N. et al. Nitrogen cycles: past, present, and future. *Biogeochemistry* **70**, 153–226 (2004).
- McIsaac, G. F., David, M. B., Gertner, G. Z. & Goolsby, D. A. Nitrate flux in the Mississippi River. *Nature* **414**, 166–167 (2001).
- Kendall, C., Elliott, E. M., & Wankel, S. D. in *Stable Isotopes in Ecology and Environmental Science* (2007).
- Radikova, Z. et al. Possible effects of environmental nitrates and toxic organochlorines on human thyroid in highly polluted areas in Slovakia. *Thyroid* **18**, 353–362 (2008).
- Shearer, L. A., Goldsmith, J. R., Young, C., Kearns, O. A. & Tamplin, B. R. Methemoglobin levels in infants in an area with high nitrate water supply. *Am. J. Public Health* **62**, 1174–1180 (1972).
- Schullehner, J., Hansen, B., Thygesen, M., Pedersen, C. B. & Sigsgaard, T. Nitrate in drinking water and colorectal cancer risk: a nationwide population-based cohort study. *Int. J. Cancer* **143**, 73–79 (2018).
- Steffen, W. et al. Sustainability. Planetary boundaries: guiding human development on a changing planet. *Science* **347**, 1259855 (2015).
- Fadhullah, W., Yaccob, N. S., Syakir, M. I., Muhammad, S. A., Yue, F. J. & Li, S. L. Nitrate sources and processes in the surface water of a tropical reservoir by stable isotopes and mixing model. *Sci. Total Environ* **700**, 134517 (2020).
- Luu, T. N. M., Do, T. N. & Matiatos, I. et al. Stable isotopes as an effective tool for N nutrient source identification in a heavily urbanized and agriculturally intensive tropical lowland basin. *Biogeochemistry* **149**, 17–35 (2020).
- Matiatos, I. Nitrate source identification in groundwater of multiple land-use areas by combining isotopes and multivariate statistical analysis: a case study of Asopos basin (Central Greece). *Sci. Total Environ* **541**, 802–814 (2016).
- Wassenaar, L. I. Evaluation of the origin and fate of nitrate in the Abbotsford Aquifer using the isotopes of ^{15}N and ^{18}O in NO_3^- . *Appl. Geochem.* **10**, 391–405 (1995).
- Zhang, Y., Li, F., Zhang, Q., Li, J. & Liu, Q. Tracing nitrate pollution sources and transformation in surface- and ground-waters using environmental isotopes. *Sci. Total Environ* **490**, 213–222 (2014).
- Altabet, M. A., Wassenaar, L. I., Douence, C. & Roy, R. A Ti(III) reduction method for one-step conversion of seawater and freshwater nitrate into N_2O for stable isotopic analysis of $^{15}\text{N}/^{14}\text{N}$, $^{18}\text{O}/^{16}\text{O}$ and $^{17}\text{O}/^{16}\text{O}$. *Rapid Commun. Mass Spectrom.* **33**, 1227–1239 (2019).
- Kendall C. in *Isotope Tracers in Catchment Hydrology* (1998).
- Xue, D. et al. Present limitations and future prospects of stable isotope methods for nitrate source identification in surface- and groundwater. *Water Res.* **43**, 1159–1170 (2009).
- Briand, C. et al. Legacy of contaminant N sources to the NO_3^- signature in rivers: a combined isotopic $\delta^{15}\text{N}-\text{NO}_3^-$, $\delta^{18}\text{O}-\text{NO}_3^-$, $\delta^{11}\text{B}$ and microbiological investigation. *Sci. Rep.* **7**, 41703 (2017).
- Fenech, C., Rock, L., Nolan, K., Tobin, J. & Morrissey, A. The potential for a suite of isotope and chemical markers to differentiate sources of nitrate contamination: a review. *Water Res.* **46**, 2023–2041 (2012).
- Widory, D., Kloppmann, W., Chery, L., Bonnin, J., Rochdi, H. & Guinamant, J. L. Nitrate in groundwater: an isotopic multi-tracer approach. *J. Contam. Hydrol.* **72**, 165–188 (2004).
- Granger, J. & Wankel, S. D. Isotopic overprinting of nitrification on denitrification as a ubiquitous and unifying feature of environmental nitrogen cycling. *Proc. Natl Acad. Sci. USA* **113**, E6391–E6400 (2016).
- Nestler, A. et al. Isotopes for improved management of nitrate pollution in aqueous resources: review of surface water field studies. *Environ. Sci. Pollut. Res. Int.* **18**, 519–533 (2011).
- Soto, D. X., Koehler, G., Wassenaar, L. I. & Hobson, K. A. Spatio-temporal variation of nitrate sources to Lake Winnipeg using N and O isotope ($\delta^{15}\text{N}$, $\delta^{18}\text{O}$) analyses. *Sci. Total Environ* **647**, 486–493 (2019).
- Vystavna, Y. et al. Small-scale chemical and isotopic variability of hydrological pathways in a mountain lake catchment. *J. Hydrol.* **585**, 124834 (2020).
- Goody, D. C., Macdonald, D. M., Lapworth, D. J., Bennett, S. A. & Griffiths, K. J. Nitrogen sources, transport and processing in peri-urban floodplains. *Sci. Total Environ.* **494–495**, 28–38 (2014).
- Kaushal, S. S., Groffman, P. M., Band, L. E., Elliott, E. M., Shields, C. A. & Kendall, C. Tracking nonpoint source nitrogen pollution in human-impacted watersheds. *Environ. Sci. Technol.* **45**, 8225–8232 (2011).
- Amundson, R. et al. Global patterns of the isotopic composition of soil and plant nitrogen. *Glob. Biogeochem. Cycles* **17**, 1031 (2003).
- Craine, J. M. et al. Convergence of soil nitrogen isotopes across global climate gradients. *Sci. Rep.* **5**, 8280 (2015).
- Handley, L. L. et al. The ^{15}N natural abundance ($\delta^{15}\text{N}$) of ecosystem samples reflects measures of water availability. *Funct. Plant Biol.* **26**, 185 (1999).
- Martinelli, L. A. et al. Nitrogen stable isotopic composition of leaves and soil: tropical versus temperate forests. *Biogeochemistry* **46**, 45–65 (1999).
- Nikolenko, O., Jurado, A., Borges, A. V., Knller, K. & Brouyre, S. Isotopic composition of nitrogen species in groundwater under agricultural areas: a review. *Sci. Total Environ.* **621**, 1415–1432 (2018).
- Suchy, M., Wassenaar, L. I., Graham, G. & Zebarth, B. High-frequency NO_3^- isotope ($\delta^{15}\text{N}$, $\delta^{18}\text{O}$) patterns in groundwater recharge reveal that short-term changes in land use and precipitation influence nitrate contamination trends. *Hydrol. Earth Syst. Sci.* **22**, 4267–4279 (2018).
- Venkiteswaran, J. J., Boeckx, P. & Goody, D. C. Towards a global interpretation of dual nitrate isotopes in surface waters. *J. Hydrol. X* **4**, 100037 (2019).
- Hoskins, A. J., Bush, A., Gilmore, J., Harwood, T. & Hudson, L. N. et al. Downscaling land-use data to provide global 30'' estimates of five land-use classes. *Ecol. Evol.* **6**, 3040–3055 (2016).
- West S. G., Finch J. F. & Curran P. J. *Structural Equation Models with Nonnormal Variables: Problems and Remedies* (1995).
- Umezawa, Y. et al. Sources of nitrate and ammonium contamination in groundwater under developing Asian megacities. *Sci. Total Environ.* **404**, 361–376 (2008).
- Venkiteswaran, J. J., Wassenaar, L. I. & Schiff, S. L. Dynamics of dissolved oxygen isotopic ratios: a transient model to quantify primary production, community respiration, and air-water exchange in aquatic ecosystems. *Oecologia* **153**, 385–398 (2007).
- Cavari, B. Z., Allen, D. A. & Colwell, R. R. Effect of temperature on growth and activity of *Aeromonas* spp. and mixed bacterial populations in the Anacostia River. *Appl. Environ. Microbiol.* **41**, 1052–1054 (1981).
- Rivett, M. O., Buss, S. R., Morgan, P., Smith, J. W. & Bemment, C. D. Nitrate attenuation in groundwater: a review of biogeochemical controlling processes. *Water Res.* **42**, 4215–4232 (2008).
- Wang, L., Butcher, A. S., Stuart, M. E., Goody, D. C. & Bloomfield, J. P. The nitrate time bomb: a numerical way to investigate nitrate storage and lag time in the unsaturated zone. *Environ. Geochem. Health* **35**, 667–681 (2013).
- Moore, T. A. et al. Prevalence of anaerobic ammonium-oxidizing bacteria in contaminated groundwater. *Environ. Sci. Technol.* **45**, 7217–7225 (2011).
- Clark, I., Timlin, R., Bourbonnais, A., Jones, K., Lafleur, D. & Wickens, K. Origin and fate of industrial ammonium in anoxic ground water- ^{15}N evidence for anaerobic oxidation (anammox). *Groundw. Monit. Remed.* **28**, 73–82 (2008).
- Follett, R. F. & Hatfield, J. L. Nitrogen in the environment: sources, problems, and management. *Sci. World J.* **1**, 920–926 (2001).
- Snider, D. M., Spoelstra, J., Schiff, S. L. & Venkiteswaran, J. J. Stable oxygen isotope ratios of nitrate produced from nitrification: (^{18}O)-labeled water incubations of agricultural and temperate forest soils. *Environ. Sci. Technol.* **44**, 5358–5364 (2010).
- Ascott, M. J. et al. Global patterns of nitrate storage in the vadose zone. *Nat. Commun.* **8**, 1416 (2017).
- Mariotti, A., Landreau, A. & Simon, B. ^{15}N isotope biogeochemistry and natural denitrification process in groundwater: application to the chalk aquifer of northern France. *Geochim. Cosmochim. Acta* **52**, 1869–1878 (1988).

45. Romanelli, A., Soto, D. X., Matiatos, I., Martinez, D. E. & Esquiú, S. A biological and nitrate isotopic assessment framework to understand eutrophication in aquatic ecosystems. *Sci. Total Environ.* **715**, 136909 (2020).
46. Böttcher, J., Strelow, O., Voerkelius, S. & Schmidt, H.-L. Using isotope fractionation of nitrate-nitrogen and nitrate-oxygen for evaluation of microbial denitrification in a sandy aquifer. *J. Hydrol.* **114**, 413–424 (1990).
47. Hotchkiss, E. R. & Hall, R. O. Jr. High rates of daytime respiration in three streams: Use of $\delta^{18}\text{O}_2$ and O_2 to model diel ecosystem metabolism. *Limnol. Oceanogr.* **59**, 798–810 (2014).
48. Wassenaar, L. I., Venkiteswaran, J. J., Schiff, S. L. & Koehler, G. Aquatic community metabolism response to municipal effluent inputs in rivers quantified using diel $\delta^{18}\text{O}$ values of dissolved oxygen. *Can. J. Fish. Aquat. Sci.* **67**, 1232–1246 (2010).
49. Davies, P. M., Bunn, S. E., & Hamilton, S. K. *Tropical Stream Ecology* (2008).
50. Parker, S. R., Poulson, S. R., Gammons, C. H. & DeGrandpre, M. D. Biogeochemical controls on diel cycling of stable isotopes of dissolved O_2 and dissolved inorganic carbon in the Big Hole River, Montana. *Environ. Sci. Technol.* **39**, 7134–7140 (2005).
51. Buchwald, C., Santoro, A. E., McIlvin, M. R. & Casciotti, K. L. Oxygen isotopic composition of nitrate and nitrite produced by nitrifying cocultures and natural marine assemblages. *Limnol. Oceanogr.* **57**, 1361–1375 (2012).
52. Angert, A., Luz, B. & Yakir, D. Fractionation of oxygen isotopes by respiration and diffusion in soils and its implications for the isotopic composition of atmospheric O_2 . *Glob. Biogeochem. Cycles* **15**, 871–880 (2001).
53. Wassenaar, L. I. & Hendry, M. J. Dynamics and stable isotope composition of gaseous and dissolved oxygen. *Ground Water* **45**, 447–460 (2007).
54. Boshers, D. S., Granger, J., Tobias, C. R., Bohlke, J. K. & Smith, R. L. Constraining the oxygen isotopic composition of nitrate produced by nitrification. *Environ. Sci. Technol.* **53**, 1206–1216 (2019).
55. Mader, M., Schmidt, C., van Geldern, R. & Barth, J. A. C. Dissolved oxygen in water and its stable isotope effects: a review. *Chem. Geol.* **473**, 10–21 (2017).
56. Fogel M. L., Cifuentes L. A. *Topics in Geobiology* (1993).
57. Brookshire, E. N. J., Hedin, L. O., Newbold, J. D., Sigman, D. M. & Jackson, J. K. Sustained losses of bioavailable nitrogen from montane tropical forests. *Nat. Geosci.* **5**, 123–126 (2012).
58. Mayer, B. & Wassenaar, L. I. Isotopic characterization of nitrate sources and transformations in Lake Winnipeg and its contributing rivers, Manitoba, Canada. *J. Great Lakes Res.* **38**, 135–146 (2012).
59. Price, P. B. & Sowers, T. Temperature dependence of metabolic rates for microbial growth, maintenance, and survival. *Proc. Natl Acad. Sci. USA* **101**, 4631–4636 (2004).
60. Mariotti, A. et al. Experimental-determination of nitrogen kinetic isotope fractionation - some principles - illustration for the denitrification and nitrification processes. *Plant Soil* **62**, 413–430 (1981).
61. Loo, S. E., Ryan, M. C., Zebarth, B. J., Kuchta, S. H., Neilsen, D. & Mayer, B. Use of $\delta^{15}\text{N}$ and $\delta^{18}\text{O}$ values for nitrate source identification under irrigated crops: a cautionary vadose zone tale. *J. Environ. Qual.* **46**, 528–536 (2017).
62. Savard, M. M., Paradis, D., Somers, G., Liao, S., & van Bochove, E. Winter nitrification contributes to excess NO_3^- in groundwater of an agricultural region: a dual-isotope study. *Water Resour. Res.* **43**, W06422 (2007).
63. Clark, I. D. & Fritz, P. *Environmental Isotopes in Hydrogeology* (1997).
64. Du, E. A database of annual atmospheric acid and nutrient deposition to China's forests. *Sci Data* **5**, 180223 (2018).
65. Beck, H. E., Zimmermann, N. E., McVicar, T. R., Vergopolan, N., Berg, A. & Wood, E. F. Present and future Koppen-Geiger climate classification maps at 1-km resolution. *Sci Data* **5**, 180214 (2018).
66. Coplen, T. B., Qi, H., Revesz, K., Casciotti, K., & Hannon J. E. in *Techniques and Methods* (2007).
67. American Public Health Association. *Standard Methods for the Examination of Water and Wastewater* 3–37 (1998).
68. Davis, J. C. & Sampson, R. J. *Statistics and Data Analysis in Geology* (1986).
69. Draper, N. R. & Smith, H. *Applied Regression Analysis* (1998).
70. R Core Team. *R Team: A Language and Environment for Statistical Computing*. <https://www.R-project.org> (2018).

Acknowledgements

The research was partly funded by the International Atomic Energy Agency (IAEA) through the Coordinated Research Project (CRP) F32007. Thanks to C. Douance and L. Poeltenstein for conducting nitrate isotope and water isotope measurements. Argentina: Acknowledges support of the National Scientific and Technical Research Council-CONICET [PIP 0350] and National Agency for Scientific and Technological Promotion [PICT 1147/17]. Canada: Acknowledges the support of the Natural Sciences and Engineering Research Council of Canada (NSERC), [RGPIN-2018-06389]. Chile: Acknowledges project ANID/FONDAP/15130015. China: Acknowledges the support of the National Key R&D Program of China (Grant # 2016YFA0601002). Finland: Acknowledges the support of the Academy of Finland funding (Grant # 287469). Italy: Acknowledges the support of the Cariplo Foundation (INTEGRON Project, Grant # 2015-0263). Malaysia: Acknowledges the support of Universiti Sains Malaysia's short-term grant (USM) [304/PTEKIND/6315079] and assistance from Kerian District Department of Drainage and Irrigation Malaysia. UK: Acknowledges the support of NERC National Capability funding and the permission of the Director of the British Geological Survey. USA: Acknowledges the Atmospheric and Geospace Sciences National Science Foundation Postdoctoral Fellowship (AGS 1624618). Vietnam: The sampling and analysis conducted in Vietnam were partly funded by the UKRI GCRF Living Deltas Hub under Grant Reference NE/S008926/1.

Author contributions

I.M. and L.I.W. conceived and wrote the paper. I.M. and L.R.M. undertook the formal analysis and visualization of the work. J.J.V., D.C.G., P.B., and E.S. discussed the results and provided critical reviews and edits of the final manuscript. F.-J.Y., G.M., C.A.-H., C.B., L.B., N.V.E., W.F., J.R.F., A.G., N.K., S.-L.L., M.T.N.L., S.P., V.R., D.S.R., A.R., P.S., F.T., D.A.T., W.W., and N.W. contributed to the review and editing of the final manuscript.

Competing interests

The authors declare no competing interests.

Additional information

Supplementary information The online version contains supplementary material available at <https://doi.org/10.1038/s43247-021-00121-x>.

Correspondence and requests for materials should be addressed to I.M.

Peer review information Primary handling editor: Teresa Ortnor

Reprints and permission information is available at <http://www.nature.com/reprints>

Publisher's note Springer Nature remains neutral with regard to jurisdictional claims in published maps and institutional affiliations.



Open Access This article is licensed under a Creative Commons Attribution 4.0 International License, which permits use, sharing, adaptation, distribution and reproduction in any medium or format, as long as you give appropriate credit to the original author(s) and the source, provide a link to the Creative Commons license, and indicate if changes were made. The images or other third party material in this article are included in the article's Creative Commons license, unless indicated otherwise in a credit line to the material. If material is not included in the article's Creative Commons license and your intended use is not permitted by statutory regulation or exceeds the permitted use, you will need to obtain permission directly from the copyright holder. To view a copy of this license, visit <http://creativecommons.org/licenses/by/4.0/>.

© The Author(s) 2021